A Comprehensive Error Analysis of Free-Space Techniques for Extracting the Permeability and Permittivity of Materials Using Reflection-Only Measurements

Raenita A. Fenner[1, *] and Mili Shah[2]

Abstract—The electromagnetic characterization of layered materials is applicable to many different applications. In previous work it has been shown that reflection-only techniques — which vary the underlying structure of the sample stack to obtain two independent measurements — are a variation of a single unifying scheme such that there is a single set of closed-form unifying extraction equations for the electric permittivity and magnetic permeability. In this paper, the error propagation method is applied to this single set of closed-form extraction equations in order to derive an accompanying set of closed-form equations to predict the measurement uncertainty of electric permittivity and magnetic permeability. An error analysis is performed on the layer-shift method, and results are compared to a Monte Carlo simulation to prove the viability of the general error analysis equations.

1. INTRODUCTION

Within the study of electromagnetics, material characterization is the determination of the relative electric permittivity, ϵ_r, and relative magnetic permeability, μ_r, through free space, waveguide, or probe measurements. The electromagnetic characterization of materials has many different applications. In medical applications, the electromagnetic characterization of materials is used for the monitoring of physiological events in the human body [1], the characterization of benign and malignant breast tissues [2], breast cancer detection [3], and studying the influence of microwaves on the human body [4]. Within the design of electronic circuits, material characterization has been used to design high-quality polymers for terahertz components [5] and to perform quality assurance of silicon wafers for integrated circuit design [6]. In agriculture and quality control of food, material characterization has been used to determine physical properties (i.e., moisture content, bulk density, and temperature) of cereal grain and seed [7] and contamination detection in cheddar cheese and beef [8]. Also, material characterization is vital in propagation analysis of mm-wave indoor networks [9] and characterization of construction materials [10].

In many material characterization applications, a frequency domain, nonresonant characterization method is required to extract ϵ_r and μ_r over a range of frequencies. Free-space reflection-only methods are often highly desired because of their simple measurement setup and the fact that transmission measurements are not required.

In [11] it was shown that all reflection-only methods that obtain two measurements by adjusting the stack behind the material under test (MUT) are variations of one single scheme that unifies all such reflection-only material characterization methods. Moreover, [11] derived a single set of closed-form extraction equations to extract ϵ_r and μ_r for all reflection-only methods that adjust the stack behind the MUT.

The closed-form extraction equations in [11] have been cited in many applications. In [12] and [13], the extraction equations are used in the fabrication of ultra-porous and lightweight epoxy foam composites. The extraction equations were used by [14] and [15] to determine the relative permittivity of fabricated foam composites for microwave absorbers. Similarly, [16] uses the extraction equations to characterize optically-reconfigurable metasurfaces.

The contribution and novelty of this paper is a set of closed-form equations to perform the error analysis for all reflection-only methods that adjust the stack behind the MUT; these equations are termed the *general error analysis equations*. Based on the wide use of the extraction equations in [11], the general error analysis equations derived in this paper will be useful to many applications, especially in the design and fabrication of metamaterials and microwave absorbers.

This paper will first review the closed-form extraction equations for ϵ_r and μ_r from [11]. Next, the general error analysis equations are n derived and described. Lastly, an error analysis is performed for the layer-shift method to prove the random propagated error predicted by the general error analysis equations which is comparable to the random propagated error predicted by a Monte Carlo simulation.

2. REVIEW OF FREE SPACE REFLECTION-ONLY EXTRACTION EQUATIONS

Free space reflection-only techniques necessitate a layered-planar sample illuminated by an incident field and the reflection coefficient of the sample measured with a vector network analyzer (VNA). Two independent measurements of the reflection coefficient are required if both ϵ_r and μ_r need to be determined. Generally, the two independent measurements can be obtained by either altering the incident field or altering the layered sample stack of the material under test (MUT). An example technique which alters the incident field is the dual-polarization technique where the reflection coefficient is measured when the incident field is at parallel polarization and a second time when the incident field is at perpendicular polarization [17]. Methods which alter the sample stack may vary the position of the sample within the stack or the composition of the adjacent layers *behind* the MUT. Examples of techniques which alter the sample stack include:

- Air/conductor backed method [18] where one measurement is made with the MUT backed by air and a second measurement when the MUT is backed by conductor.
- Layer-shift method [19] where one measurement is made with the MUT directly adjacent to a conductor and a second measurement made with the conductor shifted some distance away from the MUT with a known material sample in between the two.
- Two-thickness method [20] where two measurements are conducted with two different thicknesses of the MUT which is backed by a conductor in both instances.

Free space reflection-only material characterization techniques are illustrated with a unifying geometry shown in Figure 1. A transverse magnetic (TM) or transverse electric (TE) incident wave originates in free space and is initially incident on the overlay region in Region 1. It has been proven in [21] that methods which manipulate the overlay region will not yield two independent measurements and thus extract ϵ_r and μ_r. Therefore, it is assumed throughout this work that Region 1 is free space. The MUT, in Region 2, is assumed to be homogeneous and isotropic with permittivity ϵ_{2r} and permeability μ_{2r}. Behind the MUT is the underlay in Region 3 with permittivity and permeability profiles $\epsilon_3(z)$ and $\mu_3(z)$. The underlay can be one of several configurations including layered-homogeneous materials, spatially varied layers of materials, etc. Note that to implement these methods, the measurements should be calibrated so that the phase reference for both reflection coefficients is at the front face of the MUT.

The free space permittivity and permeability extraction equations in [11] are

$$\epsilon_{2r} = \frac{k_{z2}\eta_0}{k_0 Z_2} \qquad \mu_{2r} = \frac{k_{z2}^2 + k_0^2 \sin^2 \theta_0}{k_0^2 \epsilon_{2r}} \tag{1}$$

for TM waves and

$$\mu_{2r} = \frac{k_{z2} Z_2}{k_0 \eta_0} \qquad \epsilon_{2r} = \frac{k_{z2}^2 + k_0^2 \sin^2 \theta_0}{k_0^2 \mu_{2r}} \tag{2}$$
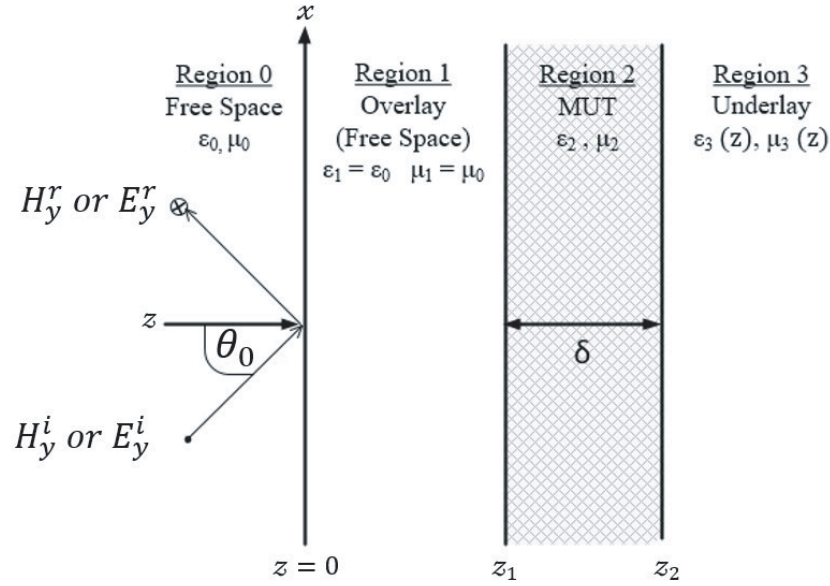
Figure 1. A general configuration of a layered planar stack including the MUT (Region 2) and adjacent layers in front and behind the MUT in Region 1 and Region 3. Electrical, magnetic, and dimensional properties are known for the material layers in Region 1 and Region 3.

for TE waves, where $\eta_0 = \sqrt{\mu_0/\epsilon_0}$ is the intrinsic impedance of free space, and $k_0 = \omega\sqrt{\mu_0\epsilon_0}$ is the wave number in free space.

Moreover, Z_2 is the wave impedance in Region 2 of Figure 1 and is defined as

$$Z_2^2 = \frac{Z_1^A Z_1^B \left(Z_3^B - Z_3^A\right) - Z_3^A Z_3^B \left(Z_1^B - Z_1^A\right)}{\left(Z_3^B - Z_3^A\right) - \left(Z_1^B - Z_1^A\right)\big)}; \tag{3}$$

and k_{z2} is the z-component of the wave vector in Region 2 of Figure 1 and is defined as

$$\tan(k_{z2}\delta) = jZ_2 \frac{Z_3^A - Z_1^A}{Z_2^2 - Z_3^A Z_1^A} = jZ_2 \frac{Z_3^B - Z_1^B}{Z_2^2 - Z_3^B Z_1^B}. \tag{4}$$

Here,

$$Z_1^A = Z_0 \frac{1 + \Gamma_0^A}{1 - \Gamma_0^A} \qquad Z_1^B = Z_0 \frac{1 + \Gamma_0^B}{1 - \Gamma_0^B} \tag{5}$$

and

$$Z_3^A = \frac{j}{\omega\epsilon_3(z_2)} \frac{\left(f_3^A(z_2)\right)' - \Gamma_3\left(g_3^A(z_2)\right)'}{f_3^A(z_2) - \Gamma_3 g_3^A(z_2)} \qquad Z_3^B = \frac{j}{\omega\epsilon_3(z_2)} \frac{\left(f_3^B(z_2)\right)' - \Gamma_3\left(g_3^B(z_2)\right)'}{f_3^B(z_2) - \Gamma_3 g_3^B(z_2)}. \tag{6}$$

are the wave impedances in Regions 1 and 3, respectively. It is assumed that the properties of Regions 1 and 3 are known, and two measurements of the Fresnel reflection coefficient, Γ_0, have been performed. The two measurements of Γ_0 are indicated with superscripts A and B which correspond to the two unique underlay regions required. Additionally, Z_0 is the characteristic impedance of free space and also the characteristic impedance of Region 1 in Figure 1. For TM polarization $Z_0 = \eta_0 \cos\theta_0$ and for TE polarization $Z_0 = \eta_0/\cos\theta_0$.

Note that $Z_3^{A,B}$ in Eq. (6) are left in terms of the general forward and backward travelling waves, $f_3(z) = e^{-jk_{z3}z}$, $g_3(z) = e^{jk_{z3}z}$, and the z-component of the wave vector in Region 3, k_{z3}, until the specific configuration of underlays is determined. For instance, in the case of both TM and TE polarizations, if the underlay is a perfect electric conductor (PEC) then $Z_3^{A,B} = 0$. For a homogeneous

material, $Z_3^{A,B} = \mathsf{Z_3}$. In the case of a homogeneous material which is then terminated by a PEC, $Z_3^{A,B} = j\mathsf{Z_3}\tan(k_{z3}(z_3 - z))$ with $z_2 \le z \le z_3$.

The derivations of Eqs. (1) and (2) are based on the continuity of the transverse impedances in the MUT and adjacent regions. For the complete derivations of Eqs. (1) and (2), the reader is referred to [11]. Note that in Eqs. (1,2), ϵ_0 and μ_0 are directly substituted because Region 1 is assumed to be free space as depicted in Figure 1.

3. GENERAL ERROR ANALYSIS EQUATIONS

An error analysis is performed to establish the impact of random error on an experimentally determined quantity. Random error is inherently present in all measurements and is due to unpredictable fluctuations in reading of measurement apparatus. To predict the random error propagated into ϵ_r and μ_r, the standard approach defined by [22] is utilized. Specifically, the random error is defined as

$$\sigma_{\epsilon_{2r}} = \sqrt{\left(\sigma_\theta \frac{\partial \epsilon_r}{\partial \theta}\right)^2 + \left(\sigma_\delta \frac{\partial \epsilon_r}{\partial \delta}\right)^2 + \left(\sigma_{|\Gamma_0|} \frac{\partial \epsilon_r}{\partial |\Gamma_0|}\right)^2 + \left(\sigma_{\angle \Gamma_0} \frac{\partial \epsilon_r}{\partial \angle \Gamma_0}\right)^2} \tag{7}$$

for ϵ_r and

$$\sigma_{\mu_{2r}} = \sqrt{\left(\sigma_\theta \frac{\partial \mu_r}{\partial \theta}\right)^2 + \left(\sigma_\delta \frac{\partial \mu_r}{\partial \delta}\right)^2 + \left(\sigma_{|\Gamma_0|} \frac{\partial \mu_r}{\partial |\Gamma_0|}\right)^2 + \left(\sigma_{\angle \Gamma_0} \frac{\partial \mu_r}{\partial \angle \Gamma_0}\right)^2} \tag{8}$$

for μ_r.

The independent variables are angle, θ, sample thickness, δ, magnitude of the reflection coefficient, $|\Gamma_0|$, and phase of the reflection coefficient, $\angle \Gamma_0$.

3.1. General Error Analysis Equations for TM Polarization

Assume that a TM polarized wave is used as the incident wave to interrogate the sample stack in Figure 1 and measure the reflection coefficient, Γ_0. The extraction of the MUT's ϵ_r and μ_r is performed with the equations in Eq. (1). The random propagated error in Eqs. (7) and (8) must be determined chiefly by finding the first derivatives of ϵ_r and μ_r with respect to θ, δ, $|\Gamma_0|$, and $\angle \Gamma_0$. Seeing that ϵ_r and μ_r in Eq. (1) are closed-form expressions, the first derivatives for Eqs. (7) and (8) will be in closed-form as well.

First, let x represent any one of the independent variables θ, δ, $|\Gamma_0|$, or $\angle \Gamma_0$. By use of the quotient rule, the first-derivatives of ϵ_r and μ_r with respect to x are

$$\frac{\partial \epsilon_{2r}}{\partial x} = \frac{\eta_0}{k_0} \left[\frac{\mathsf{Z_2} \partial k_{z2}/\partial x - k_{z2} \partial \mathsf{Z_2}/\partial x}{\mathsf{Z_2^2}}\right] \tag{9}$$

and

$$\frac{\partial \mu_{2r}}{\partial x} = \frac{\epsilon_{2r}\left(2k_{z2}\partial k_{z2}/\partial x + 2k_0^2 \sin\theta_0 \partial \sin\theta_0/\partial x\right) - \left(k_{z2}^2 + k_0^2 \sin^2\theta_0\right)\partial \epsilon_{2r}/\partial x}{k_0^2 \epsilon_{2r}^2} \tag{10}$$

For simplification, redefine $\mathsf{Z_2}$ as

$$\mathsf{Z_2} = \sqrt{\mathsf{Z_{2A}}} \qquad \text{where} \qquad \mathsf{Z_{2A}} = \frac{Z_{2B}Z_{2C} - Z_{2D}Z_{2E}}{\left(Z_3^B - Z_3^A\right) - \left(Z_1^B - Z_1^A\right)} \tag{11}$$

where $Z_{2B} = Z_1^A Z_1^B$, $Z_{2C} = Z_3^B - Z_3^A$, $Z_{2D} = Z_3^A Z_3^B$, and $Z_{2E} = Z_1^B - Z_1^A$. The first derivative of $\mathsf{Z_2}$ can then be generally redefined as

$$\frac{\partial \mathsf{Z_2}}{\partial x} = \frac{1}{2\sqrt{\mathsf{Z_{2A}}}} \frac{\partial \mathsf{Z_{2A}}}{\partial x} \tag{12}$$

with

$$
\begin{aligned}
\frac{\partial \mathsf{Z}_{2A}}{\partial x} &= \frac{1}{\left((Z_3^B - Z_3^A) - (Z_1^B - Z_1^A)\right)^2} \left((Z_3^B - Z_3^A - (Z_1^B - Z_1^A))\right) \\
&\quad \times \left(Z_{2B}\frac{\partial Z_{2C}}{\partial x} + Z_{2C}\frac{\partial Z_{2B}}{\partial x} - Z_{2E}\frac{\partial Z_{2D}}{\partial x} - Z_{2D}\frac{\partial Z_{2E}}{\partial x}\right) \\
&\quad - (Z_{2B}Z_{2C} - Z_{2D}Z_{2E}) \times \left(\frac{\partial Z_3^B}{\partial x} - \frac{\partial Z_A}{\partial x} - \frac{\partial Z_1^B}{\partial x} + \frac{\partial Z_1^A}{\partial x}\right)
\end{aligned} \tag{13}
$$

Here

$$
\frac{\partial Z_{2B}}{\partial x} = Z_1^B\frac{\partial Z_1^A}{\partial x} + Z_1^A\frac{\partial Z_1^B}{\partial x} \qquad \frac{\partial Z_{2C}}{\partial x} = \frac{\partial Z_3^B}{\partial x} - \frac{\partial Z_3^A}{\partial x} \tag{14}
$$

$$
\frac{\partial Z_{2D}}{\partial x} = Z_3^B\frac{\partial Z_3^A}{\partial x} + Z_3^A\frac{\partial Z_3^B}{\partial x} \qquad \frac{\partial Z_{2E}}{\partial x} = \frac{\partial Z_1^B}{\partial x} - \frac{\partial Z_1^A}{\partial x} \tag{15}
$$

and $\partial Z_1^{A,B}/\partial x$ is defined as

$$
\frac{\partial Z_1^{A,B}}{\partial x} = \eta_0 \left[\Gamma_m^{A,B}\frac{\partial \cos \theta_0}{\partial x} + \cos \theta_0\frac{\partial \Gamma_m^{A,B}}{\partial x}\right] \tag{16}
$$

where

$$
\Gamma_m^{A,B} = \frac{1 + \Gamma_0^{A,B}}{1 - \Gamma_0^{A,B}} \qquad \frac{\partial \Gamma_m}{\partial x} = \frac{2\angle\Gamma_0}{(1 + \Gamma_0)^2} \qquad \frac{\partial \Gamma_m}{\partial x} = \frac{2|\Gamma_0|}{(1 + \Gamma_0)^2}. \tag{17}
$$

$\partial Z_3^{A,B}/\partial x$ in Eqs. (14) and (15) are left undefined until the specific configuration of the underlay region (Region 3 in Figure 1) is defined. Now that $\partial \mathsf{Z}_2/\partial x$ has been defined, $\partial k_{z2}/\partial x$ must also be defined to complete the definition of Eqs. (9) and (10). Again for simplicity and clarity, redefine k_{z2} as

$$
k_{z2} = \frac{1}{\delta}\mathrm{atan}\,(j\mathsf{Z}_2\phi) \qquad \phi = \frac{Z_3^{A,B} - Z_1^{A,B}}{\mathsf{Z}_2^2 - Z_3^{A,B}Z_1^{A,B}} \tag{18}
$$

The first derivative of k_{z2} is then

$$
\frac{\partial k_{z2}}{\partial x} = \frac{\partial}{\partial x}\left\{\frac{1}{\delta}\right\}\mathrm{atan}\,(j\mathsf{Z}_2\phi) + \frac{1}{\delta}\left(\frac{1}{1 + (j\mathsf{Z}_2\phi)^2}\right)\frac{\partial\,(j\mathsf{Z}_2\phi)}{\partial x} \tag{19}
$$

where

$$
\begin{aligned}
\frac{\partial\,(j\mathsf{Z}_2\phi)}{\partial x} &= j\phi\frac{\partial \mathsf{Z}_2}{\partial x} + \left(\frac{j\mathsf{Z}_2}{(\mathsf{Z}_2^2 - Z_3^B Z_1^B)^2}\right) \\
&\quad \times \left((\mathsf{Z}_2^2 - Z_3^B Z_1^B)\left(\frac{\partial Z_3^B}{\partial x} - \frac{\partial Z_1^B}{\partial x}\right) - (Z_3^B - Z_1^B)\left(2\mathsf{Z}_2\frac{\partial \mathsf{Z}_2}{\partial x} - \left(Z_3^B\frac{\partial Z_1^B}{\partial x} + Z_1^B\frac{\partial Z_3^B}{\partial x}\right)\right)\right).
\end{aligned} \tag{20}
$$

Thus, a practitioner simply needs to compute $\partial Z_1/\partial x$ and $\partial Z_3/\partial x$ for both underlay configurations A and B to subsequently compute Eqs. (9) and (10).

3.2. General Error Analysis Equations for TE Polarization

The general error analysis equations for a TE incident wave are largely unchanged from the equations for TM waves in Section 3.1. The first derivatives of ϵ_{2r} and μ_{2r} are defined as

$$
\frac{\partial \mu_{2r}}{\partial x} = \frac{1}{\eta_0 k_0}\left(\mathsf{Z}_2\frac{\partial k_{z2}}{\partial x} + k_{z2}\frac{\partial \mathsf{Z}_2}{\partial x}\right) \tag{21}
$$

and

$$
\frac{\partial \epsilon_{2r}}{\partial x} = \frac{\mu_{2r}\left(2k_{z2}\partial k_{z2}/\partial x + 2k_0^2 \sin \theta_0\partial \sin \theta_0/\partial x\right) - \left(k_{z2}^2 + k_0^2 \sin^2 \theta_0\right)\partial \mu_{2r}/\partial x}{k_0^2\mu_{2r}^2} \tag{22}
$$

The remaining definitions of $\partial \mathsf{Z}_2/\partial x$, Z_{22A}, $\partial k_{z2}/\partial x$, etc. are the same as defined in Section 3.1.

3.3. Generic Methodology for the General Error Analysis Equations

A summary of how to use the equations derived in Sections 3.1 and 3.2 to determine σ_{ϵ_r} and σ_{μ_r} for a single independent variable is likely useful for practitioners. A general method to use the error analysis equations derived in Sections 3.1 and 3.2 includes:

(i) Compute the wave impedances Z_1^A, Z_1^B, Z_3^A, and Z_3^B defined in Eqs. (5) and (6) using the measured reflection coefficients, characteristic impedance, and knowledge of the two underlay configurations. The user should also compute $\partial Z_1^A/\partial x$ and $\partial Z_1^B/\partial x$ using Eq. (16), as well as $\partial Z_3^A/\partial x$, and $\partial Z_3^B/\partial x$.

(ii) Next, the practitioner should use Z_1^A, Z_1^B, Z_3^A, and Z_3^B to determine Z_{2B}, Z_{2C}, Z_{2D}, and Z_{2E} defined in Section 3.1.

(iii) Find $\partial Z_{2B}/\partial x$, $\partial Z_{2C}/\partial x$, $\partial Z_{2D}/\partial x$, and $\partial Z_{2E}/\partial x$ in Eqs. (14) and (15) using Z_1^A, Z_1^B, Z_3^A, Z_3^B, $\partial Z_1^A/\partial x$, $\partial Z_1^B/\partial x$, $\partial Z_3^A/\partial x$, and $\partial Z_3^B/\partial x$.

(iv) Find Z_{2A}, $\partial Z_{2A}/\partial x$, and $\partial Z_2/\partial x$ using Eqs. (11), (13), and (12), respectively.

(v) Determine ϕ with Eq. (18), $\partial j\mathsf{Z}_2\phi/\partial x$ with Eq. (20), and $\partial k_{z2}/\partial x$ with Eq. (19).

(vi) Compute σ_{ϵ_r} with Eq. (7) and σ_{μ_r} with Eq. (8) using $\partial\epsilon_r/\partial x$ (with Eq. (9) for TM polarization and Eq. (22) for TE polarization) and $\partial\mu_r/\partial x$ (with Eq. (10) for TM polarization and Eq. (21) for TE polarization).

4. ERROR ANALYSIS OF THE THE LAYER SHIFT METHOD

To prove that the general error analysis equations derived in Sections 3.1 and 3.2 will predict accurate propagated uncertainty an error analysis has been performed on the *layer-shift method*. The free space setup of the layer-shift method is shown in Figure 2. In the layer-shift method Γ_0^A is measured when the MUT is directly adjacent to a PEC, and Γ_0^B is measured when there is a homogeneous material of thickness Δ between the MUT and PEC. Additionally, now that the underlay regions have been specified, $Z_3^{A,B}$ in Eq. (6) is

$$Z_3^A = 0 \qquad Z_3^B = j\mathsf{Z}_3 \tan(k_{z3}\Delta). \tag{23}$$

as explained in Section 1.
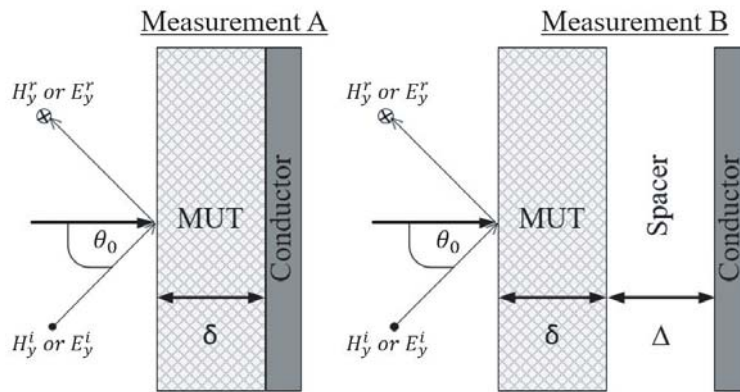
Figure 2. Diagram of the free space implementation of the *Layer Shift Method*.

In practice after the underlay configuration and Z_3^A and Z_3^B are defined, a practitioner then only needs to determine $\partial Z_3^{A,B}/\partial x$ and $\partial Z_1^{A,B}/\partial x$ for $x = \theta$, δ, $|\Gamma_0|$, and $\angle\Gamma_0$. The equations for the error analysis are presented in a fashion where all simplifications are accounted.

4.1. Propagated Uncertainty due to Measured Sample Thickness, δ

The error analysis for random propagated error due on δ is provided here. The error analysis for a single, independent variable is provided to show how the equations derived in Sections 3.1 and 3.2 are implemented. A TM wave is assumed for this example.

For uncertainty of sample thickness, x used in Eqs. (9), (10) and (21), (22) is replaced with δ. First with $Z_3^A = 0$, it follows that $Z_{2C} = Z_3^B$ and $Z_{2D} = 0$. Next, the first derivatives of $Z_3^{A,B}$ are

$$\frac{\partial Z_3^A}{\partial \delta} = 0 \qquad \frac{\partial Z_3^B}{\partial \delta} = jZ_3 k_{z3} \sec^2(k_{z3}\Delta). \tag{24}$$

Note that $k_{z3} = \sqrt{k_3^2 - k_0^2 \sin^2 \theta_0}$ has no dependence of δ and that the spacer thickness Δ is considered to contribute to the uncertainty due to sample thickness. Additionally,

$$\frac{\partial Z_1^A}{\partial \delta} = 0 \qquad \frac{\partial Z_1^B}{\partial \delta} = 0 \tag{25}$$

in (16) because $\partial \cos \theta_0 / \partial \delta = 0$ and $\partial \Gamma_m^{A,B} / \partial \delta = 0$. Subsequently, $\partial Z_{2B} / \partial \delta = 0$ in Eq. (14), $\partial Z_{2E} / \partial \delta = 0$ in Eq. (15), and Eq. (13) becomes

$$\frac{\partial Z_{2A}}{\partial \delta} = \frac{\left(Z_3^B + Z_1^A - Z_1^B\right)\left(Z_{2B} \partial Z_{2c} / \partial \delta\right) - Z_{2B} Z_{2C} \partial Z_3^B / \partial \delta}{\left(Z_3^B + Z_1^A - Z_1^B\right)^2}. \tag{26}$$

With $Z_3^A = 0$, it is easiest to write ϕ in Eq. (18) in terms of *Measurement A*; therefore, $\phi = {}^{-Z_1^A}/z_2^2$, Eq. (20) is simplified to

$$\frac{\partial (jZ_2 \phi)}{\partial \delta} = j\phi \frac{\partial Z_2}{\partial \delta} + \frac{2jZ_1^A \partial Z_2 / \partial \delta}{Z_2^2}. \tag{27}$$

With Eqs. (26) and (27) defined, everything is set to substitute into Eqs. (12) and (19) and then subsequently into Eqs. (7) and (8).

4.2. Results

A complete error analysis is performed for all of the independent variables in the free space implementation of the layer-shift method described in [11]. TM polarization is assumed.

The MUT was a sample of magnetic radar absorbing material (MagRAM) consisting of a suspension of 35% by the volume of BASF EW grade magnetic particles in a commercially available polyurethane elastomeric resin. A sample sheet of thickness $\delta = 0.1452$ cm and 60.96 cm on a side was placed on top of an aluminum plate and illuminated using a focus-beam system at an incidence angle of $\theta_0 = 40°$. The spacer for *Measurement B* is a Plexiglas sample with $\Delta = 0.5861$ cm and $\epsilon_{3r} \approx 2.66 - j0.0077$.
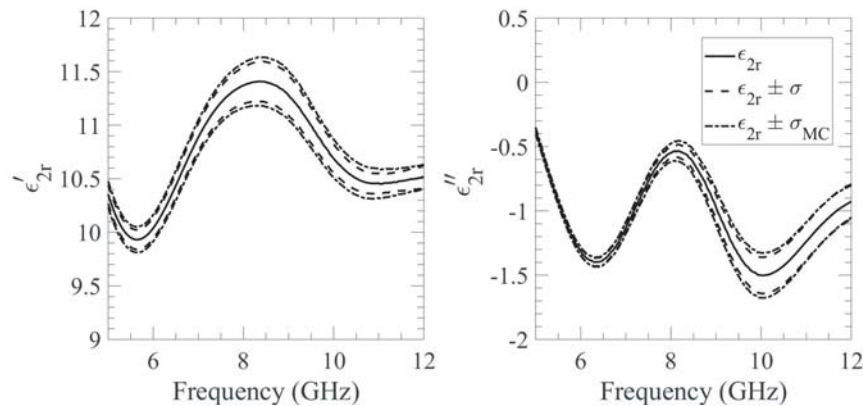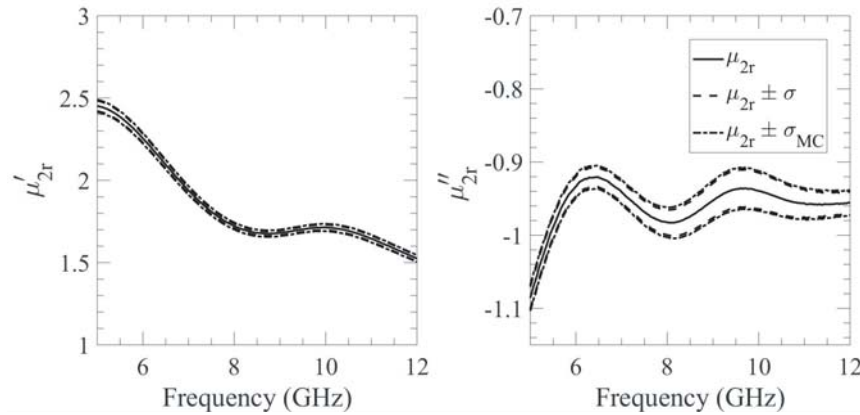

Figure 3. Extracted ϵ_{2r} and associated standard deviation predicted by the general error analysis equations and Monte Carlo simulations.

The error analysis is conducted assuming $\sigma_\theta = 0.5°$, $\sigma_\delta = 0.01\,\text{mm}$, $\sigma_{|\Gamma_0|} = 0.004$, and $\sigma_{\angle\Gamma_0} = 0.8°$. The extraction and error analysis is conducted from 5–12 GHz. The uncertainty predicted from the general error analysis presented in this paper is compared to uncertainty predicted by Monte Carlo simulation. At each frequency, 10,000 Monte Carlo trials were run.

Figure 3 shows the results of the extracted ϵ_{2r} and the associated standard deviation predicted by the general error analysis and Monte Carlo simulation; the standard deviation predicted by the general error analysis is indicated simply as σ, while the standard deviation predicted by Monte Carlo simulation is indicated as σ_{MC}.

The extracted ϵ_{2r} in Figure 3 corresponds greatly to results published in [11] which were also corroborated with a standard waveguide characterization technique. Simultaneously, $\epsilon_{2r} \pm \sigma$ and $\epsilon_{2r} \pm \sigma_{MC}$ show great agreement across the frequency band.

Figure 4 shows the results of the extracted μ_{2r} and the associated standard deviation predicted by the general error analysis and Monte Carlo simulation. The extracted μ_{2r} values correspond to those in [11]. Also, as in the case of ϵ_{2r}, there is great agreement between $\mu_{2r} \pm \sigma$ and $\mu_{2r} \pm \sigma_{MC}$.

Figure 4. Extracted μ_{2r} and associated standard deviation predicted by the general error analysis equations and Monte Carlo simulations.

5. CONCLUSION

The unifying set of closed form extraction equations for ϵ_{2r} and μ_{2r} in [11] provide a simple means for analyzing measurement error due to uncertainty in sample thickness, incidence angle, and measured s-parameters. Closed-form expressions for the sensitivity terms in the error-propagation method are derived, and uncertainty results predict comparable uncertainty to Monte Carlo simulation. The general error analysis equations are applicable to all of the techniques obtained by varying the configuration of the underlay region such as the layer-shift method and air/conductor backed method.

REFERENCES

1. Valentinuzzi, M. E., J. P. Morucci, and C. J. Felice, "Bioelectrical impedance techniques in medicine. Part II: Monitoring of physiological events by impedance," *Critical Reviews in Biomedical Engineering*, Vol. 24, Nos. 4–6, 353–466, 1996.
2. Bindu, G. and K. T. Mathew, "Characterization of benign and malignant breast tissues using 2-D microwave tomographic imaging," *Microwave and Optical Technology Letters*, Vol. 49, 2341–2345, Oct. 2007.
3. Zhang, H., S. Y. Tan, and H. S. Tan, "A novel method for microwave breast cancer detection," *Progress In Electromagnetics Research*, Vol. 83, 413–434, 2008.
4. Rosen, A., M. Stuchly, and A. Vander Vorst, "Applications of RF/microwaves in medicine," *IEEE Transactions on Microwave Theory and Techniques*, Vol. 50, No. 3, 963–974, 2002.

5. Perret, E., N. Zerounian, S. David, and F. Aniel, "Complex permittivity characterization of benzocyclobutene for terahertz applications," *Microelectronic Engineering*, Vol. 85, 2276–2281, Nov. 2008.

6. Baba, N., Z. Awang, and D. Ghodgaonkar, "A free-space method for measurement of complex permittivity of silicon wafers at microwave frequencies," *Asia-Pacific Conference on Applied Electromagnetics, 2003, APACE 2003*, 119–123, 2003.

7. Trabelsi, S. and S. O. Nelson, "Density-independent functions for on-line microwave moisture meters: A general discussion," *Measurement Science and Technology*, Vol. 9, 570–578, Apr. 1998.

8. Krraoui, H., F. Mejri, and T. Aguili, "Nondestructive measurement of complex permittivity by a microwave technique: Detection of contamination and food quality," *Journal of Electromagnetic Waves and Applications*, Vol. 31, No. 16, 1638–1657, 2017.

9. Fagiani, A., M. Vogel, and A. S. Cerqueira, "Material characterization and propagation analysis of mm-waves indoor networks," *Journal of Microwaves, Optoelectronics and Electromagnetic Applications*, Vol. 17, No. 4, 628–637, Dec. 2018.

10. Degli-Esposti, V., M. Zoli, E. M. Vitucci, F. Fuschini, M. Barbiroli, and J. Chen, "A method for the electromagnetic characterization of construction materials based on Fabry-Pérot resonance," *IEEE Access*, Vol. 5, 24938–24943, Oct. 2017.

11. Fenner, R. A., E. J. Rothwell, and L. L. Frasch, "A comprehensive analysis of free-space and guided-wave techniques for extracting the permeability and permittivity of materials using re ection-only measurements," *Radio Science*, Vol. 47, No. 1, 2012.

12. Breiss, H., A. E. Assal, R. Benzerga, A. Sharaiha, A. Jrad, and A. Harmouch, "Ultra-porous and lightweight microwave absorber based on epoxy foam loaded with long carbon fibers," *Materials Research Bulletin*, Vol. 137, 111188, May 2021.

13. Breiss, H., A. E. Assal, R. Benzerga, C. Méjean, and A. Sharaiha, "Long carbon fibers for microwave absorption: Effect of fiber length on absorption frequency band," *Micromachines*, Vol. 11, 1–18, Dec. 2020.

14. Assal, A. E., H. Breiss, R. Benzerga, A. Sharaiha, A. Jrad, and A. Harmouch, "Toward an ultra-wideband hybrid metamaterial based microwave absorber," *Micromachines*, Vol. 11, 930, Oct. 2020.

15. Pometcu, L., C. Méjean, R. Benzerga, A. Sharaiha, P. Pouliguen, and C. L. Paven, "On the choice of the dielectric characterization method for foam composite absorber material," *Materials Research Bulletin*, Vol. 96, 107–114, 2017.

16. Krraoui, H., C. Tripon-Canseliet, I. Maksimovic, S. Varault, G. Pillet, S. Maci, and J. Chazelas, "Characterization of optically-reconfigurable metasurfaces by a free space microwave bistatic technique," *Applied Sciences (Switzerland)*, Vol. 10, 4353, Jun. 2020.

17. Fenner, R., E. Rothwell, and L. Frasch, "The dual polarization method for characterization of dielectric materials," *Journal of Electromagnetic Waves and Applications*, Vol. 30, No. 3, 318–330, 2016.

18. Chen, L. F., C. K. Ong, C. P. Neo, V. V. Varadan, and V. K. Varadan, *Microwave Electronics: Measurement and Materials Characterization*, John Wiley & Sons, Nov. 2004.

19. Kalachev, A., I. Kukolev, S. Matitsin, L. Novogrudskiy, K. Rozanov, A. Sarychev, and A. Seleznev, "The methods of investigation of complex dielectric permittivity of layer polymers containing conductive inclusions," *MRS Online Proceedings Library*, Vol. 214, 1990.

20. Baker-Jarvis, J., E. Vanzura, and W. Kissick, "Improved technique for determining complex permittivity with the transmission/reflection method," *IEEE Transactions on Microwave Theory and Techniques*, Vol. 38, No. 8, 1096–1103, 1990.

21. Fenner, R. and E. J. Rothwell, "On the inadequacy of the overlay method for characterizing a conductor-backed material using free-space measurements," *2010 IEEE Antennas and Propagation Society International Symposium*, 1–4, 2010.

22. Taylor, J. and S. Taylor, *Introduction to Error Analysis: The Study of Uncertainties in Physical Measurements. ASMSU/Spartans. 4. Spartans Textbook*, University Science Books, 1997.